Applied Catalysis B: Environmental 125 (2012) 128–135

Contents lists available at SciVerse ScienceDirect

Applied Catalysis B: Environmental

journal homepage: www.elsevier.com/locate/apcatb

Enhancement of nano titanium dioxide photocatalysis in transparent coatings by polyhydroxy fullerene

Wei Bai[a,b], Vijay Krishna[a], Jie Wang[a], Brij Moudgil[a,c], Ben Koopman[a,b,*]

[a] Particle Engineering Research Center, University of Florida, Gainesville, FL, 32611, USA
[b] Department of Environmental Engineering Sciences, University of Florida, Gainesville, FL, 32611, USA
[c] Department of Materials Science and Engineering, University of Florida, Gainesville, FL, 32611, USA

ARTICLE INFO

Article history:
Received 25 February 2012
Received in revised form 14 May 2012
Accepted 22 May 2012
Available online 30 May 2012

Keywords:
Procion red MX-5B
TiO_2
UVA
Nanocomposite
Antimicrobial coatings
Aspergillus niger
Fungal spores
Fullerol
Fullerenol

ABSTRACT

Microbe transmission *via* surfaces is a common mode for the spreading of infectious diseases. A simple way to combat disease transmission *via* surfaces is to apply antimicrobial coatings. We have developed a thin, transparent, photocatalytic coating for rapid destruction of microbes. The coating uses polyhydroxy fullerene (PHF) as an enhancer for nano TiO_2 photocatalysis. A nanocomposite of PHF and TiO_2 was synthesized through physical mixing of the two components in aqueous suspension. The nanocomposite was characterized by dynamic light scattering, zeta potential and Langmuir adsorption isotherm. A coating of the PHF/TiO_2 nanocomposite was characterized by scanning electron microscopy. Photocatalytic activity of the nanocomposite coating, as indicated by degradation of organic dye (Procion red MX-5B) under UVA illumination, was optimal at a PHF/TiO_2 ratio of 0.01. The nanocomposite coating degraded the organic dye twice as fast as a coating of TiO_2 that contained no PHF. The nanocomposite coating was then applied to photocatalytically inactivate spores of *Aspergillus niger*, a household fungus commonly implicated in asthma. The nanocomposite inactivated spores three times as fast as a coating of TiO_2 containing no PHF. Changes to the morphology of *A. niger* spores due to photocatalysis were investigated using scanning electron microscopy.

1. Introduction

Microbe transmission *via* surfaces is a common mode for the spreading of infectious diseases [1]. A simple way to combat disease transmission *via* surfaces is to apply antimicrobial coatings. The ideal antimicrobial coating has the following properties:

(1) effective in killing pathogenic microorganisms;
(2) requires no toxic or hazardous chemicals for synthesis;
(3) does not alter the appearance or texture of underlying materials (*i.e.*, transparent);
(4) activated by agents that are readily available, such as light;
(5) inexpensive.

Ultraviolet-A (UVA) active, photocatalytic coatings based on titanium dioxide (TiO_2) have the potential to satisfy all of these criteria. Furthermore, they also destroy organic pollutants such as volatile organic compounds and are self-cleaning. To achieve thin, transparent coatings that are also antimicrobial, it is important to maximize the efficiency of the photocatalyst in converting light energy to chemical energy.

A number of approaches have been devised to improve the efficiency of TiO_2 photocatalysis under UVA illumination. Doping or forming nanocomposites with noble metals (Pt, Au and Ag) [2–4], metal ions [5], metal oxide [6], carbon nanotubes [7,8], graphene oxide [9], fullerene [10,11] and polyhydroxy fullerene [12,13] enhances photocatalytic efficiency. However, doping or nanocomposite formation typically requires a sol–gel process, which is energy-intensive, requires toxic chemicals and is expensive. In contrast, nanocomposites of polyhydroxy fullerene (PHF) and TiO_2 form spontaneously through self-assembly when the two components are mixed. Krishna et al. [12,13] demonstrated that PHF/TiO_2 nanocomposite in aqueous suspension photocatalytically degraded organic dye 2.6 times faster and inactivated *Escherichia coli* 1.9 times faster than TiO_2 alone. They showed that PHF physically adsorbs on TiO_2, and postulated that the adsorbed PHF serves as an electron scavenger, which facilitates electron–hole pair separation, and leads to greater production of hydroxyl radicals. Electron paramagnetic resonance spectroscopy confirmed that photocatalytic production of hydroxyl radicals was increased in

Abbreviations: PHF, polyhydroxy fullerene; TiO_2, titanium dioxide; UVA, ultraviolet A; CFU, colony forming unit.

* Corresponding author at: Department of Environmental Engineering Sciences, University of Florida, Gainesville, Florida, 32611, USA. Tel.: +1 352 392 7104; fax: +1 352 392 3076.
E-mail address: bkoop@ufl.edu (B. Koopman).

0926-3373/$ – see front matter © 2012 Elsevier B.V. All rights reserved.
http://dx.doi.org/10.1016/j.apcatb.2012.05.026

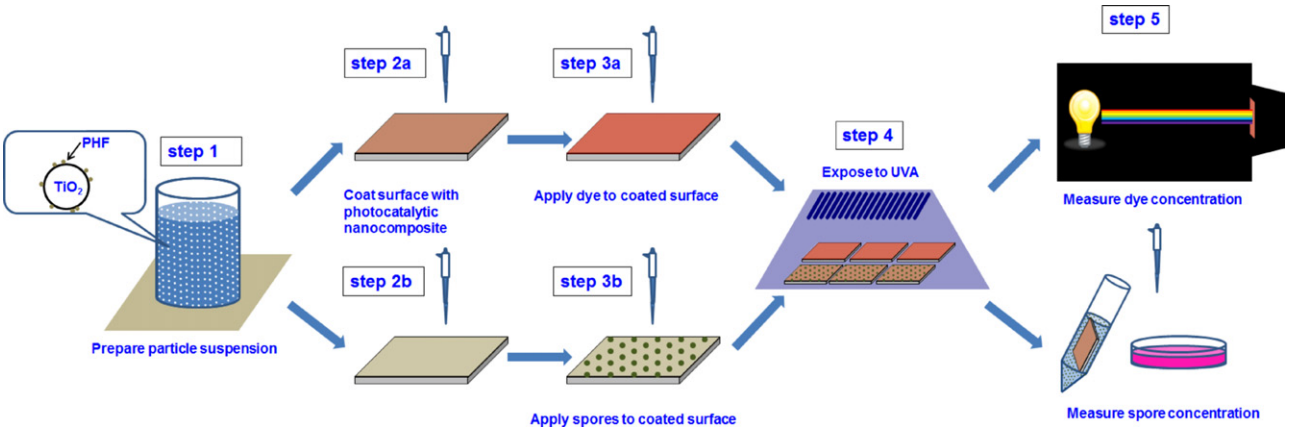

Fig. 1. Procedure for testing performance of photocatalytic coatings.

the presence of PHF [13]. Polyhydroxy fullerene is water-soluble, biocompatible and biodegradable and has been shown to possess antioxidant properties, inhibit allergic response and inhibit tumor growth [14–18]. The concentrations of PHF utilized in the PHF/TiO_2 nanocomposite are four orders of magnitude lower than the LC_{10} reported for human dermal fibroblasts [19].

Until now, the capability of PHF to enhance the photocatalytic activity of TiO_2 in a coating has not been evaluated. The objective of this study was therefore to test the effectiveness of thin, transparent coatings made of PHF/TiO_2 nanocomposite. The optimal ratio of PHF to TiO_2 for use in formulating the nanocomposite was determined using dye degradation as the performance measure. The optimized nanocomposite was then tested for inactivation of *Aspergillus niger*, a fungal species commonly occurring in both indoor and outdoor environments and frequently cited as a contributor to respiratory diseases, such as asthma [20]. *A. niger* spores are highly resistant to photocatalysis, in comparison to viruses and bacteria [21].

2. Experimental

2.1. Chemicals and reagents

Chemicals were obtained from Fisher Scientific, except as noted. Titanium dioxide (anatase, 5 nm) was obtained from Alfa Aesar (Ward Hill, MA). PHF was obtained from BuckyUSA (Houston, TX) or synthesized in our laboratory according to the protocol of Gao et al. [22]. Procion red MX-5B dye was obtained from Sigma–Aldrich Inc. (St. Louis, MO). Phosphate-buffered saline (PBS) solution was prepared by dissolving 12.36 g Na_2HPO_4, 1.80 g NaH_2PO_4 and 85.00 g NaCl in 1000 mL of deionized water and then diluting 10× immediately before use. PBS/SDS solution was prepared by adding 0.576 g sodium dodecyl sulfate (SDS) to 1000 mL of PBS and then autoclaving at 120 °C and 16 bar for 15 min.

2.2. Culturing and enumeration of A. niger spores

Asperigillus niger (ATCC 16888) were grown on potato dextrose agar for 7 days at 37 °C and then fungal spores were scraped from the agar plate with an inoculation loop and suspended in sterile deionized water. A series of 10-fold dilutions (10^{-1} to 10^{-5}) was prepared from the suspension by adding 0.333 mL of sample to 3.0 mL sterile PBS/SDS in a dilution tube, followed by vortexing for 10 s.

To enumerate the spores in a dilution, a volume of 0.1 mL was spread over sterile dichloran rose bengal chloramphenicol agar in 100 mm × 15 mm Petri dishes. The plates were inverted and then incubated at 37 °C for 24 h. Where possible, results were taken from plates that contained between 30 and 300 colonies.

2.3. Coating preparation and testing

The steps of each experiment are described below (Fig. 1).

- Step 1 – Ten mg of TiO_2 was added to a volume of 9 mL of deionized water in a 20 mL scintillation vial. The TiO_2 suspension was sonicated (Misonix Sonicator 3000, Farmingdale, NY) at the highest power level (providing 180–200 W) for 30 min total (10 min on/2 min off ×3). A volume of 1 mL of PHF solution, containing 200, 100, 50 or 0 mg/L PHF, was then added and the suspension was mixed with magnetic stirrer for 10 min.
- Step 2 – Grout was chosen as a test substrate because it is prone to fungal colonization. Grout surface was prepared by mixing grout powder (Mapei Keracolor^{TM} U, Deerfield Beach, FL) with deionized water at a 2:1 mass ratio using a spatula for 5 min, allowed to stand unmixed for 10 min, and then mixed for another 2 min. The grout-water mixture (0.15 g wet weight) was spread over a glass slide (2.5 cm × 1.8 cm) and dried overnight at room temperature. Thickness of TiO_2 coatings on grout surfaces was calculated from

$$d = \frac{cV}{\rho A f_d} \quad (1)$$

where d = calculated thickness of TiO_2 coating, c = aqueous concentration of TiO_2, V = volume of TiO_2 suspension applied to surface, ρ = density of TiO_2, A = area of surface and f_d = maximum volume fraction of randomly close packed spheres = 0.634 [23].

Ceramic tiles were used to test photocatalytic inactivation of *A. niger* spores, because commercial grout formulation contains antimicrobial agents. Tiles (2.5 cm × 2.5 cm) were obtained from American Olean Inc. (Dallas, TX). The tile surfaces were almond-colored with a matte finish. PHF/TiO_2 nanocomposite suspension was pipetted onto the grout or tile surface to give a surface loading of 64 μg/cm^2. The coated surfaces were dried overnight at room temperature. Additional tiles were coated with Stöber silica (SiO_2; Geltech) to serve as an inert control surface. SiO_2 suspension was prepared by adding 10 mg of SiO_2 to a volume of 10 mL deionized water, giving a concentration of 0.1 wt%. The suspension was sonicated as described previously. A volume of 0.4 mL of SiO_2 suspension was pipetted onto the tile surface to give a surface loading of 64 μg/cm^2.
- Step 3 – Organic dye or *A. niger* spores were applied to the test surfaces. A volume of 0.1 mL of Procion red MX-5B solution (100 mg/L) was pipetted onto coated or bare grout and allowed to spread. The dye was air dried for 1 h before testing. A volume

of 0.2 mL of *A. niger* suspension ($2–3 \times 10^5$ spores/mL) was pipetted onto each coated tile surface and allowed to spread, giving a surface loading of 6400–9600 spores/cm^2. The tiles with spores were dried in the dark in a biosafety cabinet for 24 h.

- Step 4 – The photocatalytic experiments were carried out in a chamber with 16 solar UVA lamps (320–400 nm with peak intensity at 350 nm). The UVA lamps (RPR 3500A) were purchased from Southern New England Ultra Violet Company (Branford, CT). Air was circulated in the chamber to maintain uniform temperature of 30–32 °C. Grout or tile surfaces were placed on a platform in a plastic bin (42 cm × 28 cm × 15 cm) filled to a depth of 4 cm with deionized water. The bin was covered by a plastic film in order to maintain relative humidity of 80–85%. No condensate formed on the film during the experiments. A Thermo-Hydro probe was utilized to monitor the temperature and relative humidity. The distance between samples and UVA lamps was 49.5 cm, giving an intensity of 15–17 W/m^2 under the film, which is typical of the UVA irradiance under indirect sunlight. The UVA intensity was measured by a PMA2110 detector (Solar Light Co., Glenside, PA).
- Step 5 – Performance of the photocatalytic coatings was measured by dye degradation or spore inactivation. Dye degradation was based on UV/VIS reflectance after 0, 6, 12 and 24 h of exposure to UVA. Reflectance was measured with a PerkinElmer Lambda 800 with PELA-1000 Reflectance Spectroscopy Accessory at a wavelength of 538 nm, at which absorbance of MX-5B Procion Red dye is highest. Dye degradation was calculated according to:

$$\%\text{dye degradation} = \frac{A_0 - A_t}{A_0} \times 100 \quad (2)$$

where A_0 is the calculated absorbance of dye coated on photocatalytic or bare grout surface before exposure to UVA and A_t is the absorbance of dye coated on photocatalytic or grout surface after exposure to UVA at a given time. Absorbance was calculated as the negative $\log_{10}$ of reflectance expressed as fraction. Because the color of bare grout varied somewhat, it was necessary to subtract this background color. Therefore, A_0 and A_t were calculated from

$$A_0 = A_0' - A_b \quad (3)$$

$$A_t = A_t' - A_b \quad (4)$$

where $A_{0'}$ and $A_{t'}$ are the measured absorbance of dye on grout at time zero and time t, respectively, and A_b is the measured absorbance of the bare or photocatalytically coated grout surface without dye at a given time.

Photocatalytic inactivation of *A. niger* spores was based on viable spore counts after exposure of spores on test surfaces to UVA. Spores were recovered by immersing a tile in 20 mL PBS/SDS within a polypropylene centrifuge tube and vortexing for 15 s. The tube was then sonicated at highest power for 3 min. During sonication, the tube was immersed in a flowing water bath at 28 °C. After sonication, the tube was vortexed for 15 s and the tile was removed from the centrifuge tube using a sterile forceps. The tube was then vortexed again for 15 s. The viable spores in a volume of 0.1 mL suspension from the centrifuge tube were enumerated as described previously. Inactivation was calculated from

$$\%\text{inactivation} = \frac{\text{CFU}_0 - \text{CFU}_t}{\text{CFU}_0} \times 100\% \quad (5)$$

where CFU_t is the number of colonies after time t and CFU_0 is the number of colonies at time zero.

- Step 6 – Morphological changes to *A. niger* on photocatalytic coating exposed to UVA were observed using scanning electron microscopy (JOEL 6335F FEG-SEM) at 10 kV accelerating voltage and 15 mm working distance. Because of the potentially detrimental effects of vacuum and the electron beam on spores, each tile was observed once under SEM. Hence, three different tiles with spores were prepared and then observed, one at each exposure time.

2.4. Aqueous aggregate size, zeta potential and BET surface area

Aggregate size of the nanocomposite and of TiO_2 in aqueous suspension was measured by dynamic light scattering (Nanotrac ULTRA, Microtrac, Inc. York, PA). Zeta potential was measured by doppler shift analysis (ZetaPlus, Brookhaven Instruments Corporation, Holtsville NY). Specific surface area of TiO_2 powder was measured under nitrogen using a NOVA 1200 with multipoint BET (Quantachrome Instruments, Boynton Beach, FL). TiO_2 was degassed and dried under vacuum at 110 °C for 12 h prior to measurement.

2.5. Adsorption

PHF was combined with TiO_2 as described previously in the section on coating preparation and testing. A 2 mL volume of the mixture was transferred to a centrifuge tube, followed by 30-min centrifugation at 20,800 × g. The supernatant was carefully removed by pipette and the procedure was repeated two more times. The concentration of free PHF in the final supernatant was measured by UV/vis spectroscopy at 330 nm [24,25]. The extent of adsorption was found to follow the Langmuir relationship:

$$\Gamma = \Gamma_{\max} \frac{Kc}{1 + Kc} \quad (6)$$

where Γ is the mass PHF adsorbed per mass TiO_2, c is the concentration of free PHF in equilibrium with TiO_2, $\Gamma_{\max}$ is the maximum mass PHF adsorbed per mass TiO_2 and K is the Langmuir equilibrium constant. The Langmuir parameters $\Gamma_{\max}$ and K were estimated by least squares non-linear regression.

The fraction of surface coverage of TiO_2 by PHF was calculated from

$$\text{surface coverage} = \frac{\Gamma N_A A_p}{m_p A_s} \quad (7)$$

where N_A is Avogadro's constant, A_P is the projected area of a PHF molecule (1.33 nm^2 [12], m_P is the molecular weight of PHF (1094 g/mol from the empirical formula $C_{60}(OH)_{22}$) and A_S is the specific surface area of TiO_2 (109.2 m^2/g as measured in the present study).

2.6. Data analysis

First order fits between the extent of dye degradation or spore inactivation and UVA exposure time were based on the equation

$$\ln \frac{c_t}{c_0} = kt + b \quad (8)$$

and second order fits were based on the equation

$$\frac{1}{c_t/c_0} = k't + b' \quad (9)$$

where c_t and c_0 represent absorbance or colony forming units at times t and t_0, respectively, k and k' are the reaction rate coefficients for the first and second order fits, respectively, and b and b' are arbitrary constants.

The parameter values (k, b, k', b') for the fits were determined by least squares linear regression.

One-way ANOVA and *post hoc* testing were carried out using the Dunnett's two-sided tests through NCSS statistical analysis and graphics software (NCSS, Kaysville, UT). The significance of differences between R^2 values of least square fits to experimental data was determined using the Fisher r-to-z transformation [26].

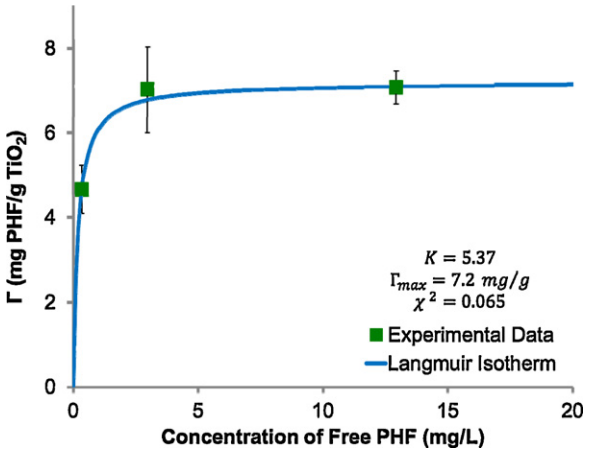

Fig. 2. Langmuir isotherm for adsorption of PHF onto TiO_2 at pH 6 and 25 °C.

3. Results

3.1. Characterization

The isotherm for adsorption of PHF on TiO_2 is given in Fig. 2. The theoretical maximum adsorption of PHF on TiO_2 was found to be 7.2 mg/g. This level was reached at a formulation ratio (g PHF added/g TiO_2) of 0.02. A decrease of the formulation ratio to 0.01 had almost no effect on the amount of PHF adsorbed, whereas dropping the formulation ratio still further to 0.005 decreased the amount of PHF adsorbed to 4.7 mg/g. The mean aggregate size of TiO_2 based on number distribution was 104 nm. This dropped to 94 nm for the nanocomposite at a formulation ratio of 0.005, and further dropped to the range of 83–86 nm at formulation ratios of 0.01 and 0.02 (Fig. 3). Zeta potential of TiO_2 was −41 mV at pH 6, compared to −48 to −49 mV for the nanocomposite (Fig. 3).

3.2. Dye degradation

TiO_2 coatings with calculated thickness ranging from 2.5 to 12.5 μm changed the color of grout surfaces from almond to white, whereas a coating with a calculated thickness of 0.25 μm had no effect on surface appearance of the grout (Fig. 4a–d). A scanning electron micrograph of the 0.25 μm thick coating shows its uniform, particulate make up. (Fig. 4e). Accordingly, a TiO_2 coating thickness of 0.25 μm was chosen for subsequent experiments. Another consideration in coating design is the effect of PHF on appearance. PHF is dark brown in color, giving PHF/TiO_2 suspensions a brown tint at higher PHF/TiO_2 ratios. To ensure that coatings remained colorless under all experimental conditions, a maximum PHF/TiO_2 weight ratio of 0.02 was established for performance testing.

Time-dependent degradation of Procion red dye on coated and bare grout is shown in Fig. 5. Under UVA exposure with photocatalyst, degradation ranged from 66% to 74% in 24 h. Without photocatalyst, degradation was 43%, which can be attributed to UVA photolysis. Almost no (4%) dye degradation was observed in the dark. PHF/TiO_2 ratios of 0.01 and 0.02 significantly ($\alpha = 0.05$) increased the extent of dye degradation at all sampling times, whereas a PHF/TiO_2 ratio of 0.005 significantly enhanced degradation only in the first 6 h. The extent of dye degradation with the nanocomposite at 6 h was almost doubled in comparison to TiO_2 alone. Based on these results, a PHF/TiO_2 ratio of 0.01 was selected for the spore inactivation study.

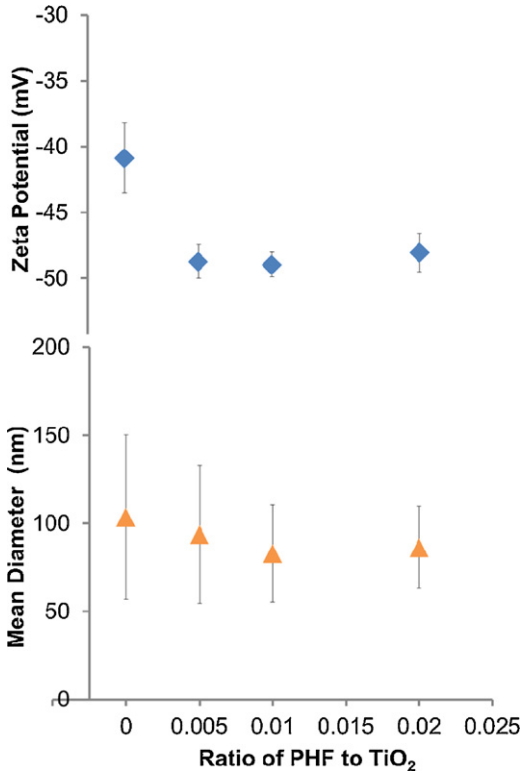

Fig. 3. Aqueous aggregate size and zeta potential of TiO_2 and PHF/TiO_2 nanocomposite.

3.3. Spore inactivation

A surface loading of 6400–9600 spores/cm^2 on the photocatalytic surface was chosen to give a sparse distribution of spores (Fig. 6), which limited spore agglomeration and thus allowed more precise enumeration of individual spores. The efficiency of spore recovery from test surfaces was evaluated by applying spores, allowing the surfaces to dry overnight in the dark, and then applying the recovery procedure. Complete recovery (within experimental error) was achieved from coatings of the nanocomposiste or TiO_2, whereas little more than half of applied spores were recovered from bare tile (Fig. 7). This result is likely due to separation of particulate coatings from the tiles during the recovery procedure, carrying the spores with them. A particulate material without photocatalytic properties, SiO_2, was therefore used as a non-photocatalytic coating. As Fig. 7 shows, complete recovery of spores was achieved from the SiO_2 coating.

The time dependent inactivation of *A. niger* spores on photocatalytic and non-photocatalytic surfaces under UVA exposure is shown in Fig. 8. A 12-h inactivation of 60% was achieved with TiO_2 alone. This was increased to 78% with the nanocomposite at a PHF/TiO_2 ratio of 0.01. Decreases in the numbers of viable spores with time on the photocatalytic surfaces paralleled decomposition of spores as imaged by scanning electron microscopy (Fig. 9). The difference in performance levels between TiO_2 alone and the PHF/TiO_2 nanocomposite was highly significant ($\alpha = 0.001$). As Fig. 8 shows, there was negligible inactivation of spores on the photocatalytic surfaces in the dark. Moderate (41% in 12 h) inactivation was observed on SiO_2 coated surfaces.

3.4. Kinetics of dye degradation and spore inactivation

Time-dependent data for dye degradation and spore inactivation were modeled by first-order and second-order least square fits,

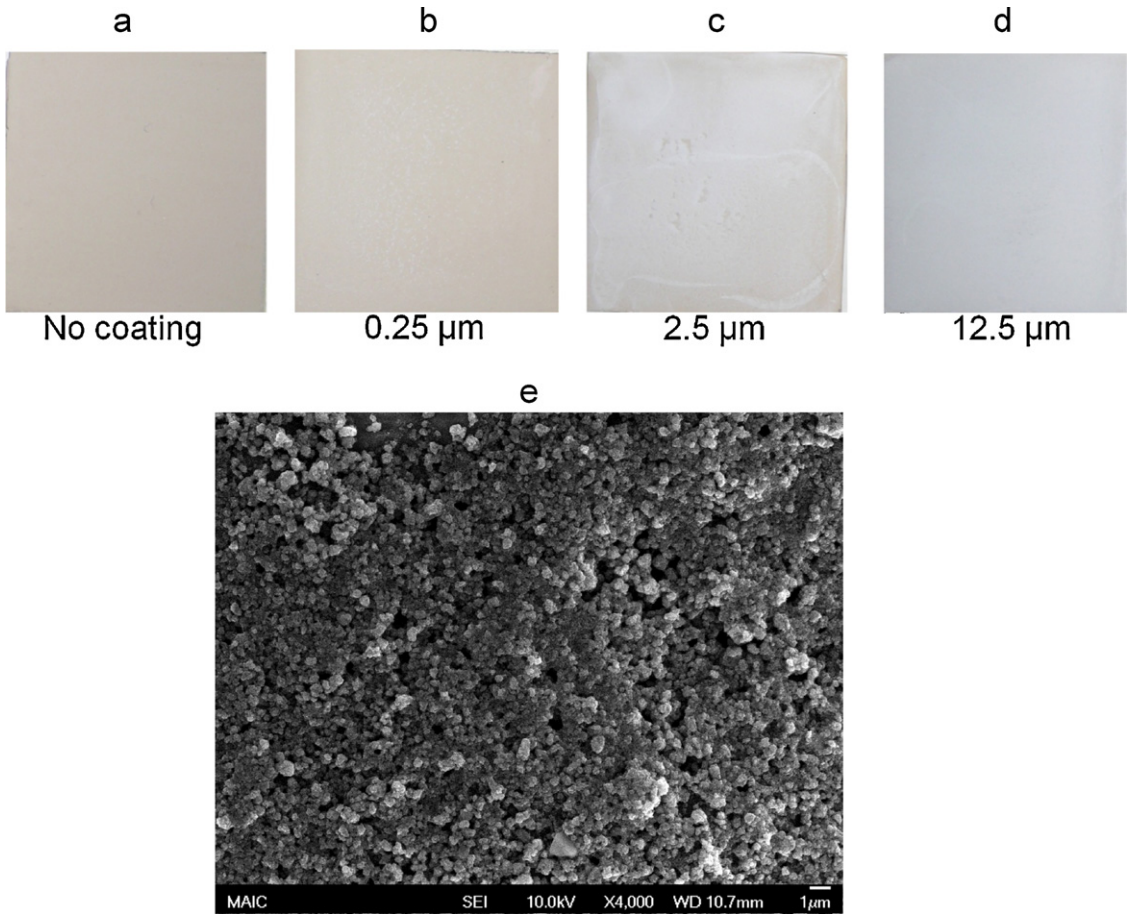

Fig. 4. (a–d) Effect of calculated TiO_2 thickness on appearance on grout surface; (e) scanning electron micrograph of TiO_2 at the thickness of 0.25 μm.

Table 1
Comparison of first-order fits and second-order fits to photocatalytic dye degradation and spore inactivation data.[a]

Contaminant	Treatment	First-order reaction kinetics		Second-order reaction kinetics		1st-order ≠ 2nd-order
		Equation	R^2	Equation	R^2	P
Dye	$PHF/TiO_2 = 0.02$	$y = -0.053x - 0.210$	0.90	$y = 0.123x + 1.153$	0.99	0.0001
	$PHF/TiO_2 = 0.01$	$y = -0.053x - 0.181$	0.92	$y = 0.123x + 1.107$	0.99	0.0006
	$PHF/TiO_2 = 0.005$	$y = -0.042x - 0.142$	0.92	$y = 0.081x + 1.099$	0.99	0.0006
	$PHF/TiO_2 = 0$	$y = -0.045x - 0.058$	0.98	$y = 0.083x + 1.005$	1.00	<0.0001
Microbes	$PHF/TiO_2 = 0.01$	$y = -0.127x + 0.048$	0.99	$y = 0.300x + 0.639$	0.95	0.0009
	$PHF/TiO_2 = 0$	$y = -0.079x - 0.007$	0.97	$y = 0.129x + 0.836$	0.95	0.29

[a] 1st-order: y is $\ln c/c_0$; 2nd-order: y is c_0/c.

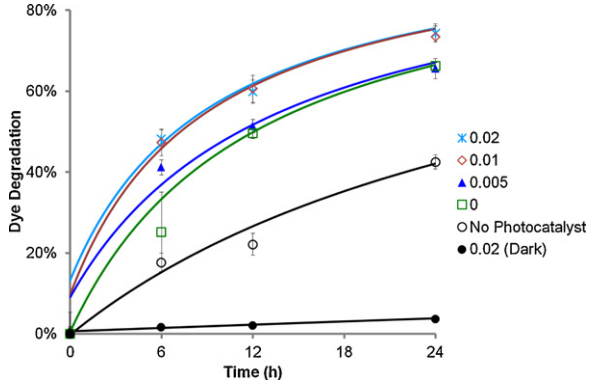

Fig. 5. Optimization of PHF/TiO_2 mass ratio (0.02, 0.01, 0.005, 0) in photocatalytic nanocomposite. Error bars represent ± 1.0 SD. (Error bars for the dark control are too small to be seen.) Model lines represent second-order fits.

as summarized in Table 1. Since the first-order and second-order equations each contain two parameters, it was possible to test the significance of the differences between R^2 values obtained with the two different equations. In modeling photocatalytic dye degradation, second-order fits were significantly better than first-order fits ($P \leq 0.0006$). Conversely, in modeling photocatalytic spore inactivation by the PHF/TiO_2 nanocomposite, the first-order fit was significantly better than the second-order fit ($P \leq 0.0009$). Kinetics of spore inactivation on TiO_2 were equally well described by either first-order or second-order fits.

The enhancements of dye degradation and spore inactivation achieved by the nanocomposite are compared in Fig. 10. In the dye degradation tests, the PHF/TiO_2 ratios of 0.01 and 0.02 give equivalent results, which are significantly better than obtained with the 0.005 ratio. In the spore inactivation experiments, the degree of variability between replicates was greater, which is not unusual when testing biological materials. As a result, there was no

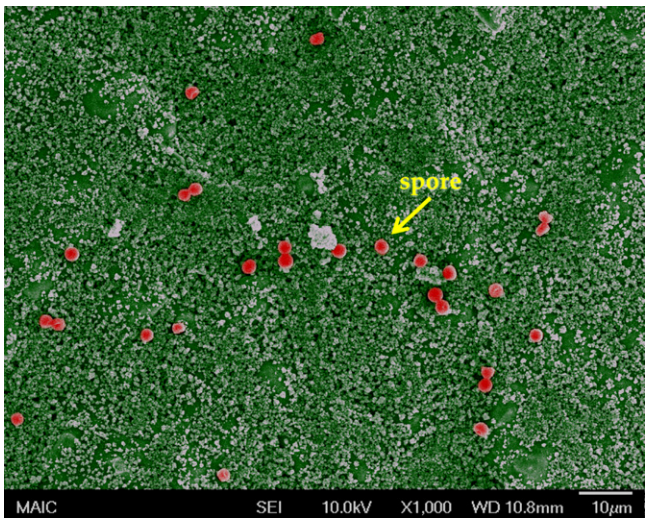

Fig. 6. False-color image of *Aspergillus niger* spores on PHF/TiO_2 nanocompsoite coating. (Spores are red spheres; coating is green background; whitish coloring indicates charging of the coating during microscopy.) (For interpretation of the references to color in this figure legend, the reader is referred to the web version of the article.)

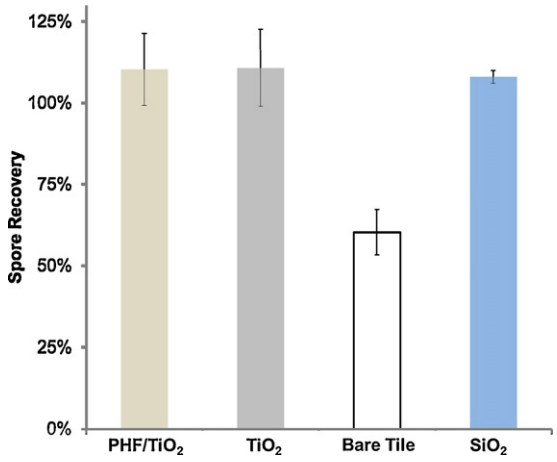

Fig. 7. Recovery of *A. niger* from test surfaces. Error bars represent ± 1.0 SD.

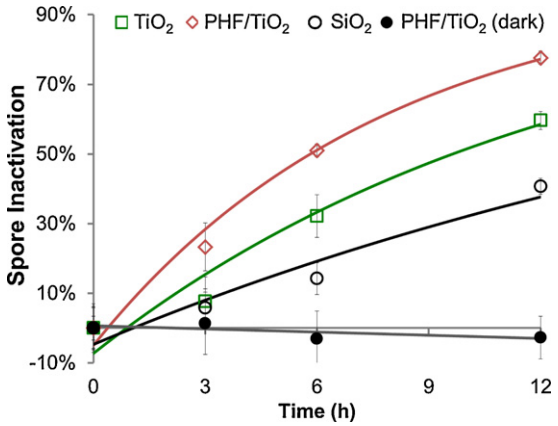

Fig. 8. Inactivation of *A. niger* spores by test surfaces. Error bars represent ± 1.0 SD. Model lines represent first-order fits.

statistical difference in the enhancement of photocatalysis achieved with nanocomposites with PHF/TiO_2 ratios of 0.005, 0.01 or 0.02.

4. Discussion

The findings of this research show that PHF enhances the performance of TiO_2 photocatalyst in thin, transparent coatings. As shown in Table 2, the 1.9 times enhancement of dye degradation achieved with the PHF/TiO_2 nanocomposite compares favorably with the enhancement ratios of 1.1–2.2 reported for other enhancers (Ag, Au, Cu, Fe, La, N, Sn, Sr). Given its comparable performance, the competitive advantage of PHF as an enhancer of photocatalysis lies in the fact that it is biocompatible, biodegradable, and the nanocomposite of PHF and TiO_2 requires no synthesis steps. The findings also raise three points for discussion: how the optimum PHF/TiO_2 ratio differs in a coating *vs.* the aqueous environment; how the kinetics of photocatalysis appear to change depending on the target component (dye *vs.* microbes); and how the observed enhancement of photocatalytic performance changes from the beginning to the end of the exposure period.

In the present study, the optimal ratio of PHF to TiO_2 was found to be 0.01, which is 10 times higher than reported by Krishna et al. [13] for aqueous suspensions of the PHF/TiO_2 nanocomposite. The adsorption isotherm developed in this study indicates that the maximum amount of PHF that can adsorb to TiO_2 is 7.2 mg/g. This corresponds to a maximum surface coverage of TiO_2 by PHF of 4.9%, which is nearly reached at a formulation ratio of 0.01 g PHF/g TiO_2 (Fig. 11). Increasing the ratio to 0.02 increases the surface coverage very slightly. Consequently, the photocatalytic activity of the

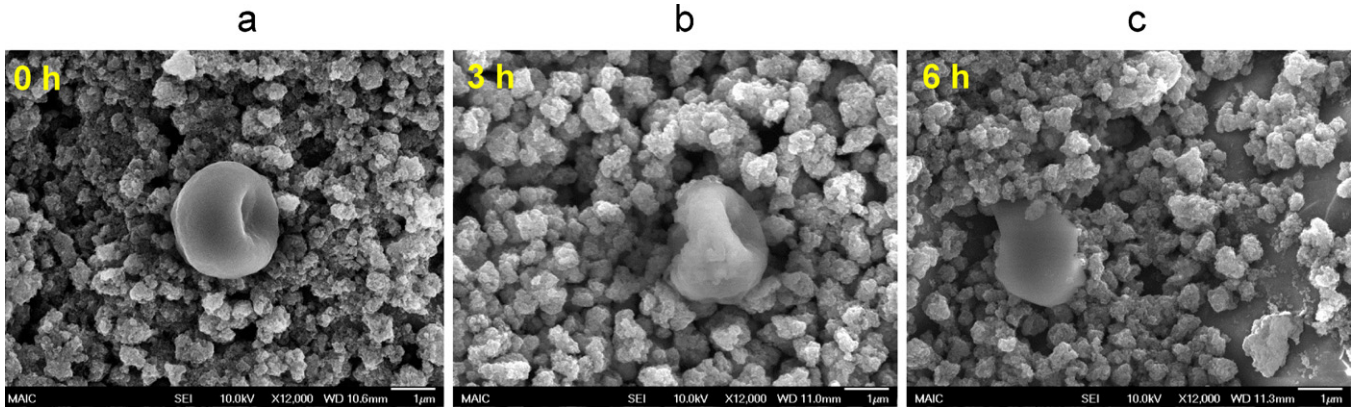

Fig. 9. Temporal changes of spore morphology on photocatalytic coatings exposed to UVA.

Table 2
Effect of enhancers on UVA photocatalytic degradation of organic dyes by TiO_2 coatings.

Study	Type of TiO_2	Enhancer	Mass ratio of enhancer to TiO_2	Model pollutant	UVA intensity (W/m^2)	Time exposed to UVA (h)	Increase in rate
This study[a]	Anatase	PHF	0.01	Procion red MX-5B	15–17	6	1.9×
Arabatzis et al. [2]	Anatase and rutile (sol–gel)	Ag	0.013	Methyl orange	0.717	1	1.8×
Arabatzis et al. [3]	Anatase and rutile (sol–gel)	Au	0.051	Methyl orange	0.717	1	2.2×
Arpac et al. [30]	Anatase (sol–gel)	Sn	0.15	Malachite Green	N/A	4	1.1×
Hermann et al. [31]	Anatase (sol–gel)	Ag		Malic acid	N/A	0.5	1.3×
Somekawa et al. [32]	Degussa P25	N		Methylene blue	N/A	N/A	1.2×
Wu et al. [33]	Anatase (sol–gel)	Fe and Au	Fe: 0.005 Au: 0.02	2,4-dichlorophenol	12.3	5	2.0×
Kumaresan et al. [34]	Anatase (sol–gel)	Sr	0.001	2,4-dinitrophenol	N/A	5	1.8×
Okte and Yilmaz [35]	Anatase (sol–gel)	La	0.0028	Methyl orange	N/A	3	1.3×
Carvalho et al. [36]	Amorphous	Cu	0.007	Methylene blue	N/A	2	1.8×

[a] The TiO_2 film was exposed to air in this study, and to water in all other studies.

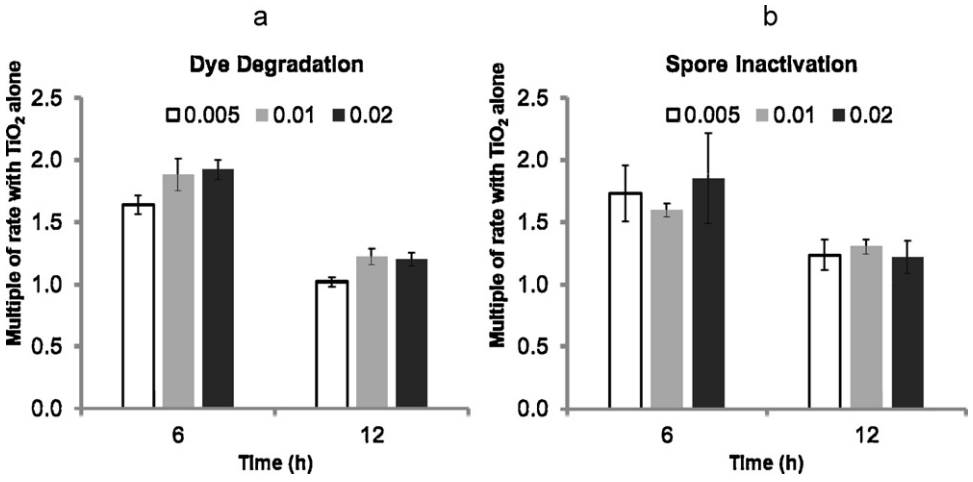

Fig. 10. Enhancement of dye degradation (a) and spore inactivation (b) by the nanocomposite at different PHF/TiO_2 ratios.

nanocomposite is not significantly increased beyond a formulation ratio of 0.01. On the other hand, dropping the ratio to 0.005 significantly decreases the surface coverage to 3.2%, which results in lower photocatalytic activity. Unlike the aqueous system studied by Krishna et al., an excess of PHF in the coating does not impair activity, because the excess simply drains from the coating and does not shade the nanocomposite.

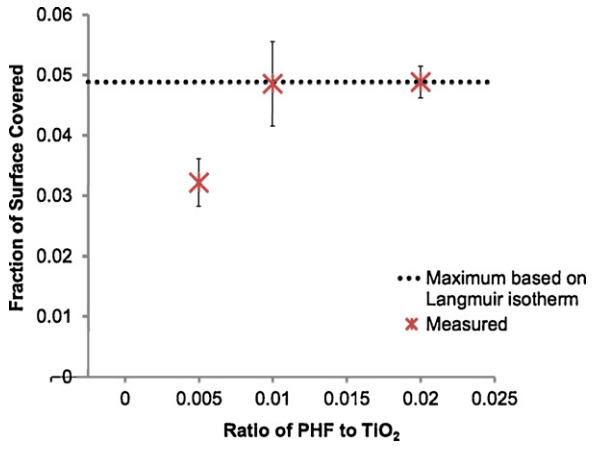

Fig. 11. Surface coverage of PHF on TiO_2 as a function of the PHF/TiO_2 formulation ratio.

Assuming that hydroxyl radical is produced at a constant rate in a photocatalytic reaction, the reaction can be theoretically considered as pseudo first order, which is supported from various studies [27,28]. However, our experimental data for photocatalytic dye degradation are better described by second-order reaction kinetics. This can be attributed to the production of colorless intermediates that accumulate during the experiment and consume hydroxyl radicals, decreasing the availability of hydroxyl radicals to unreacted dye. Hu et al. [29], using ion mass spectra, identified more than 12 intermediate products in the photocatalytic degradation of Procion red dye, all of which are capable of reacting with hydroxyl radicals.

The degree to which dye degradation and spore inactivation are enhanced by the PHF/TiO_2 nanocomposite is time dependent. At 6 h, the PHF/TiO_2 nanocomposite surface degraded nearly 2 times as much dye as TiO_2 alone, compared to 1.1× at 24 h. In the case of microbial inactivation, the nanocomposite surface inactivated 3 times as many spores as TiO_2 alone at 3 h, compared to an enhancement of 1.3× at 12 h. This relationship is expected as the remaining dye or viable spores on the surfaces approaches zero at longer exposure times.

5. Conclusion

The present study has shown that PHF enhances the UVA-photocatalytic performance of a thin, transparent TiO_2 coating by a factor of 2–3. This is achieved with a PHF/TiO_2 ratio of 0.01, at which the TiO_2 surface is nearly saturated with PHF. The enhanced performance of the PHF/TiO_2 nanocomposite was demonstrated by organic dye degradation and fungal spore inactivation. The self-assembled PHF/TiO_2 nanocomposite is very promising for use as thin, transparent, antimicrobial coatings.

Acknowledgments

Financial support from the Center for Nano-Bio Sensors and the NSF I/UCRC Center for Particulate and Surfactant Systems is gratefully acknowledged. Partial support for W. Bai was provided by a University of Florida Alumni Fellowship. Experimental work was carried out at the University of Florida Water Reclamation and Reuse Laboratory and the Particle Research Engineering Center Laboratory.

References

[1] K. Page, M. Wilson, I.P. Parkin, Journal of Materials Chemistry 19 (2009) 3819–3831.
[2] I.M. Arabatzis, T. Stergiopoulosa, M.C. Bernardc, D. Laboud, S.G. Neophytides, P.M. Falaras, Applied Catalysis B 42 (2003) 187–201.
[3] I.M. Arabatzis, T. Stergiopoulosa, D. Andreevab, S. Kitovac, S.G. Neophytides, P. Falaras, Journal of Catalysis 220 (2003) 127–135.
[4] B. Sun, A. Vorontsov, P. Smirniotis, Langmuir 19 (2003) 3151–3156.
[5] P. Bouras, E. Stathatos, P. Lianos, Applied Catalysis B 73 (2007) 51–59.
[6] A. Rampaul, I.P. Parkin, S.A. O'Neill, J. DeSouza, A. Mills, N. Elliott, Polyhedron 22 (2003) 35–44.
[7] V. Krishna, S. Pumprueg, S. Lee, J. Zhao, W. Sigmund, B. Koopman, B. Moudgil, Process Safety and Environment Protection 83 (2005) 393–397.
[8] S.H. Lee, S. Pumprueg, B. Moudgil, W. Sigmund, Colloids and Surfaces A: Biointerfaces 40 (2005) 93–98.
[9] O. Akhavan, E. Ghaderi, Journal of Physical Chemistry C 113 (2009) 20214–20220.
[10] W. Oh, F. Zhang, M. Chen, Journal of Industrial and Engineering Chemistry 16 (2010) 299–304.
[11] L. Zhang, Y. Wang, T. Xu, S. Zhu, Y. Zhu, Journal of Molecular Catalysis A: Chemical 331 (2010) 7–14.
[12] V. Krishna, N. Noguchi, B. Koopman, B. Moudgil, Journal of Colloid and Interface Science 304 (2006) 166–171.
[13] V. Krishna, D. Yanes, W. Imaram, A. Angerhofer, B. Koopman, B. Moudgil, Applied Catalysis B 79 (2008) 376–381.
[14] A. Djordjevic, J.M. Canadanovic-Brunet, M. Vojinovic-Miloradov, G. Bogdanovic, Oxidation Communication 27 (2004) 806–812.
[15] J.J. Ryan, H.R. Bateman, A. Stover, G. Gomez, S.K. Norton, W. Zhao, L.B. Schwartz, R. Lenk, C.L. Kepley, Journal of Immunology 179 (2007) 665–672.
[16] S. Trajkovic, S. Dobric, V. Jacevic, V. Dragojevic-Simic, Z. Milovanovic, A. Dordevic, Colloids and Surfaces A 58 (2007) 39–43.
[17] X. Cai, H. Jia, Z. Liu, B. Hou, C. Luo, Z. Feng, W. Li, J. Liu, Journal of Neuroscience Research 86 (2008) 3622–3634.
[18] K.M. Schreiner, T.R. Filley, R.A. Blanchette, B.B. Bowen, R.D. Bolskar, W.C. Hockaday, C.A. Masiello, J.W. Raebiger, Environmental Science and Technology 43 (2009) 3162–3168.
[19] C.M. Sayes, J.D. Fortner, W. Guo, D. Lyon, A.M. Boyd, K.D. Ausman, Y.J. Tao, B. Sitharaman, L.J. Wilson, J.B. Hughes, J.L. West, V.L. Colvin, Nano Letters 4 (2004) 1881–1887.
[20] R.E. Dales, S. Cakmak, S. Judek, T. Dann, F. Coates, J.R. Brook, R.T. Burnett, Chest 123 (2003) 745–750.
[21] A. Vohra, D.Y. Goswami, D.A. Deshpande, S.S. Block, Applied Catalysis B 64 (2006) 57–65.
[22] J. Gao, Y. Wang, K.M. Folta, V. Krishna, W. Bai, P. Indeglia, A. Georgieva, H. Nakamura, B. Koopman, B. Moudgil, PLoS ONE 6 (2011) e19976.
[23] C. Song, P. Wang, H.A. Makse, Nature 453 (2008) 629–632.
[24] Y.S. Hwang, Q. Li, Environmental Science and Technology 44 (2010) 3008–3013.
[25] L. Kong, O. Tedrow, Y.F. Chan, R.G. Zepp, Environmental Science and Technology 43 (2009) 9155–9160.
[26] R. Lowry, Concepts and Applications of Inferential Statistics. http://faculty.vassar.edu/lowry/webtext.html, 2012 (accessed 21.01.12).
[27] M.R. Hoffmann, S.T. Martin, W. Choi, W. Bahnemann, Chemical Reviews 95 (1995) 69–96.
[28] L. Hu, P.M. Flanders, P.L. Miller, T.J. Strathmann, Water Research 41 (2007) 2612–2626.
[29] C. Hu, J.C. Yu, Z. Hao, P.K. Wong, Applied Catalysis B 42 (2003) 47–55.
[30] E. Arpac, F. Sayilkan, M. Asilturk, P. Tatar, N. Kiraz, H. Sayilkan, Journal of Hazardous Materials 140 (2007) 69–74.
[31] J.M. Herrmann, H. Tahiri, Y. Ait-Ichou, G. Lassaletta, A.R. Gonzalez-Elipe, A. Fernandez, Applied Catalysis B 13 (1997) 219–228.
[32] S. Somekawa, Y. Kusumoto, M. Ikeda, B. Ahmmad, Y. Horie, Catalysis Communications 9 (2008) 437–440.
[33] Y. Wu, J. Zhang, L. Xiao, F. Chen, Applied Catalysis B 88 (2009) 525–532.
[34] L. Kumaresan, M. Mahalakshmi, M. Palanichamy, V. Murugesan, Industrial and Engineering Chemistry Research 49 (2010) 1480–1485.
[35] A.N. Ökte, Ö. Yilmaz, Applied Catalysis A 354 (2009) 132–142.
[36] H.W. Carvalho, A.P. Batista, P. Hammer, T.C. Ramalho, Journal of Hazardous Materials 184 (2010) 273–280.